Functional adjustment under lethal drought and physiological memory to water stress of two phylogenetically close and coexisting conifers

G. Gea-Izquierdo [*], D. Sánchez-Gómez, I. Aranda

ICIFOR-INIA, CSIC. Ctra. La Coruña km 7.5, 28040 Madrid, Spain

A B S T R A C T

Forest die-off can primarily affect the least drought-tolerant species and mortality be modulated by physiological legacies left by drought. To characterize the functional response and physiological memory to water stress of two phylogenetically and functionally close conifers with current contrasting field mortality and regeneration dynamics, we conducted a drought experiment in which seedlings were driven to death. Both species exhibited isohydric behavior with small hydroscapes. Yet, hydraulic performance, osmotic adjustment and gas exchange dynamics under rising water stress consistently showed that *Pinus pinea* was more resistant to drought than *Pinus pinaster*. Under water stress, *P. pinaster* exhibited greater water use efficiency, but higher photochemical damage and more constrained photosynthetic and stomatal conductance dynamics than *P. pinea*. Xylem conductivity loss under water stress and the wilting point were lower in *P. pinea*. Osmotic potential at full turgor decreased in *P. pinea* but it increased in *P. pinaster* with increasing water stress below a water potential threshold. Consequently, lethal water stress levels were higher for *P. pinea* than for *P. pinaster*. Synergistically, cumulative water stress induced physiological legacies curtailing carbon uptake and hydraulic performance in both species. Negative physiological legacies left by memory to water stress in plants, might explain delayed tree mortality years after drought. The functional responses to drought characterized agree with current field demographic dynamics under climate change in mixed evergreen forests where more drought-tolerant taxa like *P. pinea* are replacing formerly dominated *P. pinaster* stands.

1. Introduction

Drought in combination with heatwaves and increases in vapor pressure deficit under climate change are intimately linked to observed forest die-off (Brodribb et al., 2020; Breshears et al., 2021; Hammond et al., 2022). Increased mortality rates can lead to ecological substitution of plant communities (Cobb et al., 2017; Jacobsen and Pratt, 2018; Johnson et al., 2018; McDowell et al., 2020). Ecosystems dynamics greatly depend on the species capacity of acclimation to disturbances such as drought (Hudson et al., 2018; Jacobsen and Pratt, 2018; Hammond et al., 2019; Rosas et al., 2019), interlinked to other abiotic and biotic stressors along spatio-temporal gradients (Anderegg et al., 2015; Breshears et al., 2021; Trugman et al., 2021; Zandalinas and Mittler, 2022). However, we still do not entirely understand how physiological mechanisms govern forest dynamics and which functional response thresholds explain species decline. Species decline in forest dynamics under increased stress is simultaneously expressed by adult mortality and lack of regeneration. Demographic responses to stress need to be assessed concomitantly at different ontogenic stages because critical stress levels can differ along the life span of trees (Martínez-Vilalta and Lloret, 2016; Gea-Izquierdo et al., 2019; McDowell et al., 2020; Shriver et al., 2022). In this context, it is essential to better characterize the physiological mechanisms behind drought-induced increase in forest mortality rates observed globally (Trugman et al., 2021; Hartmann et al., 2022; McDowell et al., 2022).

The mechanisms explaining drought-induced mortality include complex interdependent constraints in the plant carbon and water dynamics (Adams et al., 2017; Choat et al., 2018; McDowell et al., 2020, 2022). Functional acclimation at different time scales leave legacies in physiological performance reflecting a memory of past and accumulated water stress, which complicates assessment of implication of single drought events on tree mortality (Niinemets and Keenan, 2014; Kannenberg, 2019a, 2019b; Gessler et al., 2020). To assess forest dynamics and predict die-off episodes, it is necessary to identify trait-specific response thresholds to drought (Choat et al., 2018; Hammond et al., 2019; Arend et al., 2021; Mantova et al., 2022). Forest die-off under

increasing recurrence of hot-droughts may primarily occur on the least drought-tolerant species (Niinemets and Valladares, 2006; Cobb et al., 2017; Jacobsen and Pratt, 2018; Brodribb et al., 2020). Changes in forest dynamics have been observed in mixed stands at species xeric rear-edges of their distribution, where more drought-tolerant species preferentially dominate under increasingly more xeric conditions (Woodruff et al., 2015; Martínez-Vilalta et al., 2016; Jacobsen and Pratt, 2018; Johnson et al., 2018; Gea-Izquierdo et al., 2021). Intra- and interspecific co-variation of traits shaping species drought-tolerance can be intimately related to the physiological mechanisms explaining drought-induced mortality (Mencuccini et al., 2015; Pivovaroff et al., 2016; Li et al., 2019; McDowell et al., 2022).

Carbon assimilation is intimately linked with plant hydraulics and plant-water relations (Nobel, 2009; Flexas et al., 2014; Deans et al., 2020; Joshi et al., 2022). Leaf-level physiological adjustments under water stress result in reductions in leaf area and hydraulic conductance, more stringent stomatal control of water losses, increase of non-photochemical dissipation mechanisms and damages in leaf photochemistry (Maxwell and Johnson, 2000; Niinemets and Valladares, 2006; Flexas et al., 2014; Arend et al., 2022). Consequently, carbon assimilation is constrained under water stress which in turn impacts post-drought hydraulic plant recovery (Sperry et al., 2015; Skelton et al., 2017; Kannenberg et al., 2020; Rehschuh et al., 2020). Hydraulic performance under water stress is regulated by the interplay of different mechanisms that maintain the water continuum within the plant. These mechanisms include osmoregulation, the xylem resistance to cavitation and other physiological traits defining the plant degree of isohydry (Klein, 2014; Martínez-Vilalta and Garcia-Forner, 2017; Fu and Meinzer, 2018; Hochberg et al., 2018; Lens et al., 2022). Hydraulic failure is proposed as a central mechanism involved in drought-induced tree mortality, therefore in forest die-off (Adams et al., 2017; Choat et al., 2018; Mantova et al., 2022; McDowell et al., 2022). However, tree hydraulic dysfunction can be buffered by other plant adjustments including plant hydraulic segmentation, organ-level variability in xylem vulnerability to water stress, and the capacity of osmotic adjustment of leaf wilting point (Meinzer et al., 2014; Sperry and Love, 2015; Bartlett et al., 2016; Martínez-Vilalta and Garcia-Forner, 2017; Aranda et al., 2021). Therefore, it is necessary to characterize complete functional responses along the hydraulic pathway in response to water stress to identify thresholds portending individual tree mortality (e.g. lethal water potentials, Ψ_{lethal}. Li et al., 2015; Hammond et al., 2019; Liang et al., 2021) and to inform mortality models under climate change (Sperry et al., 2015, 2019; Trugman et al., 2021; de Kauwe et al., 2022; Mantova et al., 2022).

Species substitution at the ecosystem level under climate change in mixed forests often involve species that are functionally different. However, more subtle changes between closely related species may be earlier symptoms of ecosystem changes. For example, in Mediterranean evergreen mixed forests, *Pinus pinaster* Ait. exhibits higher adult mortality and lower or total lack of regeneration rates than co-occurring species like *Pinus pinea* L., which is phylogenetically and functionally very close (Gea-Izquierdo et al., 2019; Vergarechea et al., 2019; Férriz et al., 2021). *P. pinea* can be considered more tolerant to drought than *P. pinaster* as shown by its higher resistance to xylem cavitation under water stress (Martínez-Vilalta and Piñol, 2002; Oliveras et al., 2003; Delzon et al., 2010; Battipaglia et al., 2016). Contrasting species dynamics under climate change may be explained by differences in their functional strategy under water stress. We characterized physiological performance under rising and up to lethal drought levels, and explored the existence of physiological legacies to water stress in the hydraulic and carbon functions. Seedlings of two pine species (*P. pinea* and *P. pinaster*) were experimentally set to rising water stress until plants died. Specifically, we explored differences in species performance and response thresholds during increasing water stress leading to lethal drought. We also analyzed whether past water stress impose negative memory effects in key physiological traits. In particular, we tested the

following hypotheses as likely explanations for currently observed greater success of *P. pinea* than *P. pinaster* during early life stages: (1) *P. pinea* holds higher hydraulic resistance to cavitation and higher osmoregulation capacity under water stress; (2) *P. pinea* exhibits less stringent stomatal regulation, higher photosynthetic rates, and lower photochemical damage under rising water stress; (3) cumulative drought leaves physiological legacies in the two species, i.e. longer and more intense water stress levels imprint lagged negative effects on plants curtailing hydraulic and photosynthesis performance.

2. Material and methods

2.1. Experimental setting

We conducted an experiment in which seedlings of *P. pinaster* and *P. pinea* were exposed to increasing drought levels until death was induced. Seeds of the two species were sown in plastic boxes with sand in March 2020. Once they have germinated, the seedlings were transplanted to 0.5-L pots containing a 3:1 (v/v) mixture of peat moss (Floratorf, 0–7 mm, Floragard Vertriebs GmbH, Oldenburg, Germany) and washed river sand, enriched with 2 kg m^{-3} Osmocote Plus fertilizer (16–9–12 NPK +2 micronutrients, Scotts, Heerlen, Netherlands). Seedlings were grown and maintained well-watered during one growing season in a greenhouse with temperature 15–25ºC and relative humidity 40–60%. In March 2021, one-year old seedlings were transplanted to 2-L pots with the same substrate mixture and slow release fertilizer. Plants were initially well-watered for two months to minimize transplant stress. They were then assigned to three different watering regimes (hereafter, pre-WS or water stress memory pre-conditioning) maintained for three months (June through late August), as follows: control plants (WW), watered twice a week; moderate water stressed plants (WS1), watered once a week; and severe-stressed plants (WS2), watered once every two weeks. In all cases, plants were watered to the full water holding capacity of the substrate. On September 3rd, all plants in the experiment were rehydrated to full water holding capacity. After that, irrigation was fully withdrawn from all plants. During the next three months (cycle of water deprivation to death), different functional traits were recorded at 9 evenly distributed sampling times for gas exchange and chlorophyll fluorescence parameters, and 3 evenly distributed sampling times for the pressure-volume (P-V) curves and hydraulic parameters. Measurements were stopped after three consecutive gas exchange measurements (A_n and g_s) rendered zero. This consistent zero-gas exchange point was associated to plant mortality as expressed by visual estimation of total needle dry-out and full turgor loss.

2.2. Leaf gas exchange and chlorophyll fluorescence

For every plant included in the experiment we measured leaf gas exchange and leaf chlorophyll fluorescence on light-adapted needles at a photosynthetic photon flux density (PPFD) of 1500 μmol m^2 s^{-1} using a Li-Cor 6400 portable photosynthesis system (Li-Cor, Inc. Lincoln, NE, USA) with a 6400–40 fluorescence chamber and the built-in Li-Cor 6400–01 CO_2 mixer. CO_2 concentration was set at 400 μmol mol^{-1}, leaf temperature at 22.5 ± 1.5 º C (mean ± standard deviation), relative humidity at 51.9 ± 4.0% and vapor pressure deficit (VPD) at 1.4 ± 0.1 kPa. Several fully developed needles of the most apical shoot were selected, aligned and enclosed in the cuvette gasket. Records were taken after stabilization of stomatal conductance to water vapor (g_s) to ensure stable readings. Measurements were carried out each sampling date on 6 randomly selected plants per species and pre-WS combination. The leaf area enclosed in the infrared gas analyzer (IRGA) gasket was measured on leaf scanned images (Scanner Epson Expression 12000XL, Nagano, Japan) analyzed with Fiji (Schindelin et al., 2012). Right after the gas exchange measurements, we used one FMS-2 pulse chlorophyll fluorometer (Hansatech InstrumentsLtd, King's Lynn, UK) for additional chlorophyll fluorescence measurements on ambient light-adapted

needles (PPFD of 1420 ± 122 μmol m^2 s^{-1}). Several fully developed needles adjacent to those used previously for gas exchange measurements were aligned and enclosed to cover the whole measuring area of the fluorometer leaf-clip. A final 5-second far-red pulse combined with a transient shading of the sample was applied during these chlorophyll fluorescence measurements to determine F_0' (i.e. the minimum fluorescence of a light-adapted leaf darkened for a few seconds). Leaf chlorophyll fluorescence was also assessed on the same needles after 30 min of dark-adaption.

Net photosynthesis (A_n) and g_s were obtained from gas-exchange measurements. Different photochemical and non-photochemical quenching parameters (Maxwell and Johnson, 2000; Lambers et al., 2008; Niinemets and Keenan, 2014) were obtained from chlorophyll fluorescence measurements, including the Electron transport rate (ETR), non-photochemical quenching (NPQ), photochemical quenching (qP) and the maximal efficiency of Photosystem II or quantum yield (F_v/F_m), calculated as: (1) $ETR = \left(\frac{F_m'-F_s}{F_m'}\right) fI\alpha_{leaf}$; (2) $NPQ = \frac{F_m-F_m'}{F_m'}$; (3) $qP = \frac{F_m'-F_s}{F_m'-F_0'}$; (4) $F_v/F_m = \frac{F_m-F_0}{F_m}$. Where F_m' is maximum fluorescence during a saturating light pulse of a light-adapted leaf; F_s is steady state fluorescence of a light-adapted leaf; F_0 is minimum leaf fluorescence of a dark-adapted leaf; F_m is maximum fluorescence under a saturating light pulse of a dark-adapted leaf; f is the fraction of absorbed quanta used by PSII (assumed to be 0.5 for C3 plants); I is the incident photosynthetic active radiation; and α_{leaf} is leaf absorptance.

2.3. P-V curves and leaf osmotic regulation

After each gas exchange measurement, terminal twigs with several needles were harvested in the early morning to build pressure-volume (P-V) curves. For this, 5 plants were sampled every time from each combination of species and pre-WS, resulting a total of 76 curves finally used in our analyses. Predawn (Ψ_{pd}) and midday water potentials (Ψ_{md}) were recorded on the same plants with a Scholander chamber (PMS Instrument Company, Model 1505D-EXP, Albany, OR, USA). Twigs were rehydrated before the curves were built. Pairs of balanced pressure-weight measurements were considered sequentially for each curve until completing 12–14 records (Robichaux, 1984; Aranda et al., 2021). From these measurements, we derived several water parameters: osmotic potential at full ($\Psi\pi_{full}$) and zero turgor ($\Psi\pi_{TLP}$), maximum bulk modulus of elasticity (ε_{max}), relative water content at zero turgor (RWC_0), apoplastic water fraction (relative water content in the apoplast, RWC_{apo}), and leaf ratio of saturated weight to dry weight (SW/DW). ε_{max} was estimated considering the full range of relative water content before turgor loss. The leaf capacitance before (C_{bef}) and after (C_{aft}) the wilting point were calculated as the slope of the relationship between Ψ and water losses normalized by twig dry weight. Leaf osmoregulation was analyzed along the evolution of $\Psi\pi_{full}$ under increasing water stress inferred from seedling Ψ_{pd}.

2.4. Xylem hydraulic conductivity, native embolism and hydroscape calculations

The same sampling dates for the P-V curves and after leaf gas exchange, chlorophyll fluorescence, Ψ_{pd} and Ψ_{min} had been measured, a total of 125 plants were harvested for hydraulic measurements. To measure the stringency of stomatal control under soil drying (as indirectly estimated by Ψ_{pd}), we defined species-specific hydroscapes as from Meinzer et al. (2016). To delimit the hydroscape triangle, the trajectory of Ψ_{min} as a function of Ψ_{pd} under soil drying is divided in three phases where data from Phase 2 (i.e. data associated to stomata regulation, see Fu and Meinzer, 2018) need to be distinguished. We used a novel systematic data selection procedure based on the relationship between g_s and Ψ_{min} (Klein, 2014; Knipfer et al., 2020) to establish the boundaries defining the hydroscape triangle (Appendix 1): (i) to set the point at which $\Psi_{pd} = \Psi_{min}$, we discarded data below the Ψ threshold at

which the sigmoid relationship between g_s and Ψ_{min} reaches zero, i.e. plant water potential for full stomata closure (β in Appendix 1); (ii) to eliminate from hydroscape calculations those data where variations in Ψ_{min} are likely associated to variations in irradiance and VPD (Fu and Meinzer, 2018), we discarded data points where Ψ_{min} was higher than that at 0.99 of the asymptote between g_s and Ψ_{min} assuming that this relationship follows a sigmoidal curve (Appendix 1 and 2). HAs calculated were compared with the slopes of $\Psi_{min} = a + b \cdot \Psi_{pd}$ as metrics related to the water use strategy of species (Martínez-Vilalta et al., 2014; Meinzer et al., 2016).

To measure hydraulic conductance, we cut the harvested plants under water, immediately wrapped them in wet paper and enclosed them in airtight black plastic bags to stop transpiration (Cochard et al., 2013). Once in the laboratory, stem basal segments of ~30 mm in length were cut under water and carefully debarked. Because resin may complicate hydraulic measurements in conifers (Corcuera et al., 2011; Melcher et al., 2012), three segments per plant were measured to increase robustness of the hydraulic conductance estimates (we report mean plant values). We measured the length and diameters at both ends of stem segments. Measurements of xylem embolism and hydraulic conductance were performed using XYL'EM-Plus (Xylem Embolism Meter, Bronkhorst High Tech, France) with deionized, degassed water (Liqui-Cel Mini-Module degassing membrane). We first measured initial xylem conductance (K) with a low-pressure head of 4.5 kPa. Then, we removed embolism by perfusing the segment with a high pressure of 1.75 MPa for over 10 min and then returned to the initial low pressure mode to measure maximum conductance (K_{max}) (Cochard et al., 2013; Melcher et al., 2012). This was repeated until K_{max} did not further increase. Xylem conductivity was estimated from xylem conductance by considering the length of the stem segment. Percent loss of hydraulic conductivity (PLC) caused by cavitation in the xylem was calculated as PLC= 100 * (1-K/K_{max}). For each sample, we calculated the specific hydraulic conductivity (K_s) as K/A_s (A_s = sapwood area), and the leaf-specific conductivity (K_l) as K/A_l (A_l = total plant leaf area) (Tyree and Ewers, 1991).

The relationship between PLC and Ψ_{min} was described by a sigmoidal equation commonly used to fit vulnerability curves (Pammenter and Vander Willigen, 1998): $PLC = 100 \cdot (1 + \exp(a \cdot (\Psi_{min} - P50)))^{-1}$ where a and $P50$ are constant parameters, the latter representing the pressure at which there is a 50% loss of conductivity. Additionally, we calculated the leaf-specific apparent hydraulic conductance in the soil–plant–atmosphere continuum (K_h) applying Darcy's law (Aranda et al., 2005; Nobel, 2009; Hudson et al., 2018): $K_h = \frac{E}{\Psi_s - \Psi_{min}}$, where Ψ_s and Ψ_{min} are the soil and leaf water potentials respectively and E the transpiration rate in a leaf area basis measured with the IRGA. We used Ψ_{pd} as a proxy to bulk soil water potential (Fu and Meinzer, 2018; Hochberg et al., 2018; Charrier, 2020). We calculated leaf turgor as $\Psi_P = \Psi_{min}-\Psi\pi_{TLP}$ (Nobel, 2009; Meinzer et al., 2014). Additionally, to further characterize the species water use strategy we calculated two different hydraulic safety margins (HSM. Meinzer et al., 2009; Li et al., 2019; Knipfer et al., 2020; López et al., 2021): (1) an osmotic HSM: $HSM_o = (\Psi_{\pi TLP}-P_{50})$, (2) a stomatal HSM: $HSM_{st} = (\Psi_{gs0}-P_{50})$; where $\Psi_{\pi TLP}$ are estimated values per individual and species and Ψ_{gs0} is the species water potential at full stomatal closure (see below).

2.5. Analyses of the response in functional traits to water stress

Bivariate relationships between functional traits, and between functional traits and water stress (Ψ) were assessed (Zhou et al., 2013; Knipfer et al., 2020). To address different physiological relationships, we statistically selected the best model that fitted the bivariate relationships comparing only those functions with an 'a priori' physiological theoretical basis. Different linear and non-linear relationships were compared (see Appendix 2 for more details on the functions and physiological interpretation of parameters), including: (1) *piece-wise*

regressions to test for the existence of tipping points or response thresholds in linear processes, e.g. for photochemistry and osmotic parameters as a function of Ψ_{pd}; (2) *sigmoid functions* to address non-linear relationships with physiologically meaningful horizontal maximum asymptotes (e.g. A_{n_max}, g_{s_max}), absolute minima (e.g. full stomatal closure, Ψ_{gs0} = water potential at which g_s =0, used in HSM_{st}), and inflection points (e.g. used to mimic A_n vs. Ψ_{min}); (3) *exponential functions* to address exponential relationships (e.g. K_h vs. Ψ_{min}); (4) *asymptotic exponential* relationships with horizontal asymptote and x_0 =y_0 = 0 (e.g. A_n vs. g_s). To test for differences between species and watering treatments we calculated 95% confidence intervals for the estimated linear or non-linear means of the different relationships fit. All analyses were carried out in R (R Core Team, 2020).

3. Results

3.1. Gas exchange and photochemistry under increasing water stress

P. pinaster used water more efficiently than *P. pinea* as shown by gas exchange profiles: both A_n vs. g_s (i.e. iWUE =A_n/g_s; Fig. 1A) and A_n vs. E_T (i.e. WUE =A_n/E; Beer et al., 2009; Medlyn et al., 2017. Appendix 3A). Therefore *P. pinea* was less isohydric with higher maximum stomatal conductance and transpiration rates but similar maximum A_n than *P. pinaster*. These differences in species-specific WUE were explained by higher sensitivity of leaf gas exchange (A_n and g_s) to water stress (i.e. faster decrease with decreasing water potentials) in *P. pinaster* than in *P. pinea* (Fig. 2). Complementarily, the photochemistry of *P. pinea* was more resistant to water stress than that of *P. pinaster*. The latter exhibited greater levels of non-photochemical energy dissipation and less efficient photochemistry under water stress. *P. pinea* expressed greater A_n vs. ETR than *P. pinaster* (Fig. 1), lower NPQ (Fig. 3A), less steep decrease in qP with decreasing Ψ_{pd} (Fig. 3B), and higher Fv'/Fm' (Appendix 4). In addition, *P. pinea* reached a tipping point marking a decrease in Fv/Fm with increasing water stress at lower Ψ_{pd} (Fig. 3C).

Water stress from pre-WS treatments left negative physiological legacies in seedlings. Both iWUE (Fig. 1B) and WUE (Appendix 3B) were lower in WS1 and WS2 than in WW seedlings. Maximum gas exchange (both A_n and g_s) was lower (i.e. greater fatigue) in WS2 plants, which reached full stomata closure earlier at higher water potentials than WW and WS1 plants (Fig. 2). WW reached higher A_n with lower ETR than WS2 plants. WS2 approached zero A_n faster (Fig. 1) than WW plants, because the latter kept ETR at higher levels under increasing water stress (Appendix 4c). In contrast, water stress memory did not leave legacies in the other fluorescence parameters: NPQ, qP, Fv/Fm and Fv'/Fm' were similar across pre-WS treatments (Fig. 3, Appendix 4d).

3.2. Plant-water relations under increasing water stress

P. pinea was more resistant to xylem cavitation than *P. pinaster*, as shown by lower P50 calculated using the native embolism estimates (*P. pinea,* P50 = −3.7±0.34 MPa; *P. pinaster,* P50 = −2.7±0.13 Mpa), and by consistently greater leaf-specific conductance with decreasing Ψ_{min} (Fig. 4) in *P. pinea*. There was a negative memory to water stress in hydraulic traits as shown by higher PLC and lower K_h in WS2 than in WW plants at high Ψ_{min} levels greater than ∼ − 2 MPa (Fig. 4c, d). This shows that WS2 plants had a higher initial baseline level of native xylem embolism induced by water stress during the pre-WS treatment that was not repaired by complete rewatering previous to total water deprivation in the experiment. The hydraulic safety margins were larger in *P. pinea* (HSM_o=1.6 ± 0.7 MPa; HSM_{st}=1.5 MPa) than in *P. pinaster* (HSM_o=0.9 ± 0.4 MPa; HSM_{st}=0.8 Mpa). We observed no interaction between species and pre-WS treatments for PLC (Appendix 5).

Leaf turgor was lost (i.e. negative Ψ_P) faster, and a tipping point in Ψ_P was reached earlier at higher Ψ_{min} in *P. pinaster* than in *P. pinea*. After the tipping point, Ψ_P progressively declined in both species with decreasing plant water potential (Fig. 5a). Osmoregulation capacity was higher under water stress in *P. pinea* than in *P. pinaster* (Fig. 5). Capacitance after the turgor loss point (TLP) was higher in *P. pinaster*. Remarkably, both the $\Psi\pi_{TLP}$ and $\Psi_{\pi100}$ were similar for the two species down to
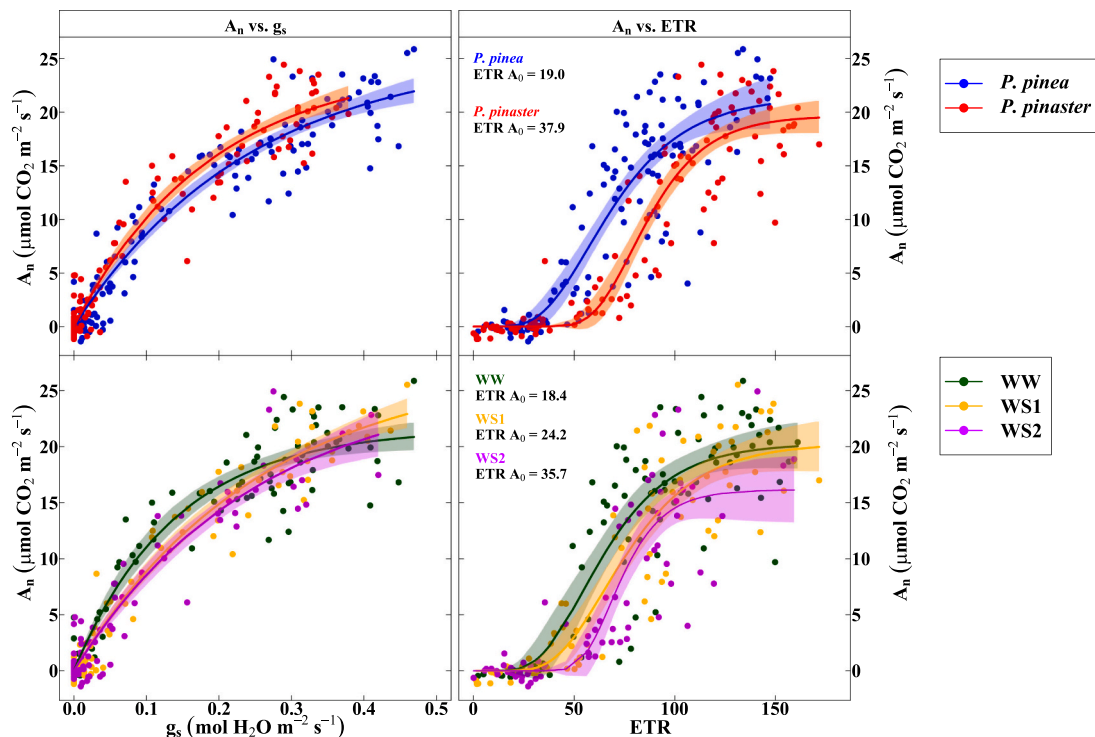
Fig. 1. Leaf photosynthesis (A_n) as a function of stomatal conductance to H_2O (g_s) in (a)-(c), and electronic transport rate (ETR) in (b)-(d). (a)-(b) show results by species, whereas (c)-(d) by water treatment. Intrinsic water-use efficiency profiles (iWUE=A_n/g_s) are thus represented in (a) and (c). WW=well-watered. WS1 =water stress 1. WS2 =water stress 2. Polygons represent 95% confidence intervals for the estimated means.
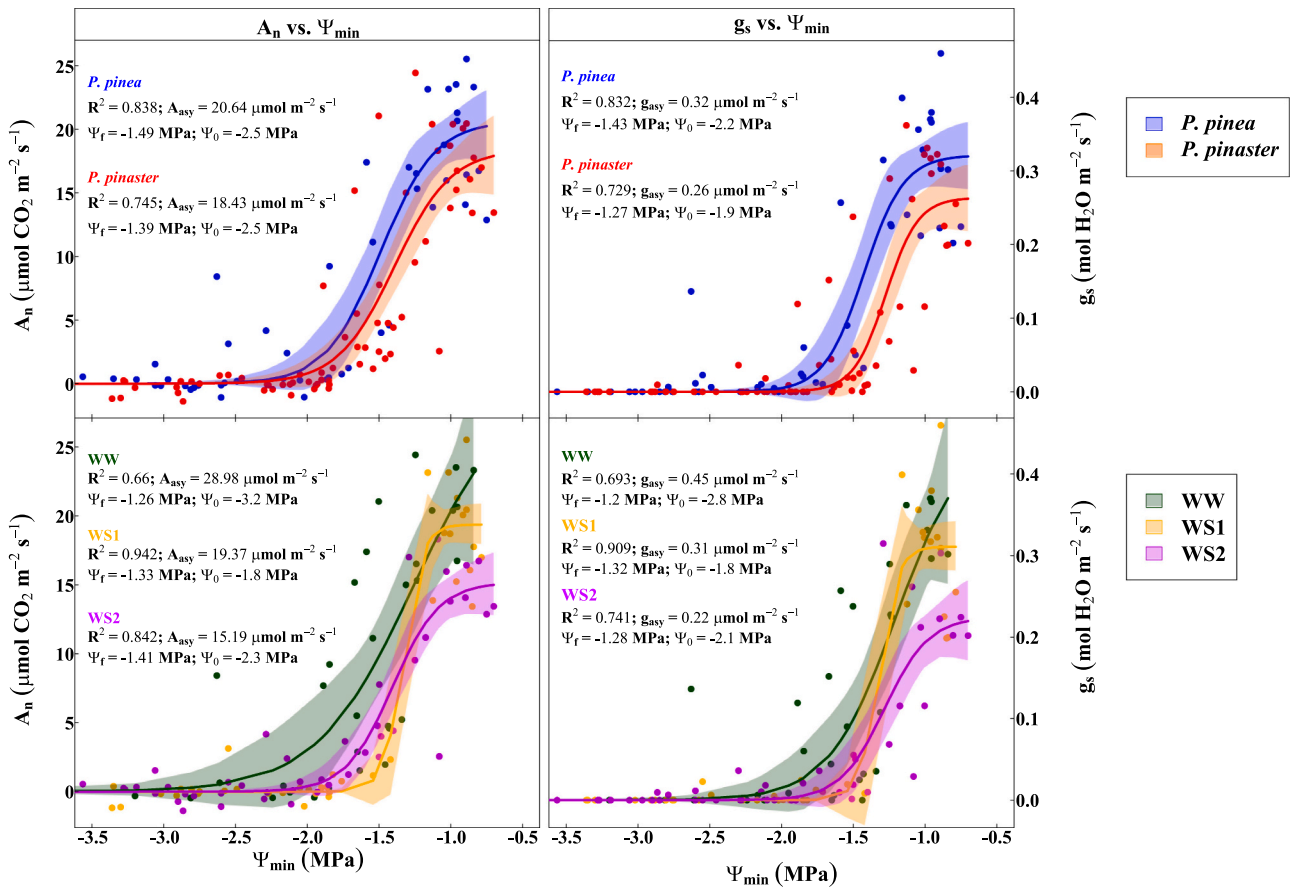
Fig. 2. Photosynthesis and stomatal conductance as a function of midday water potential (Ψ_{min}). (a)-(b) by species; (c)-(d) by water treatment. Polygons represent 95% confidence intervals for the estimated means.
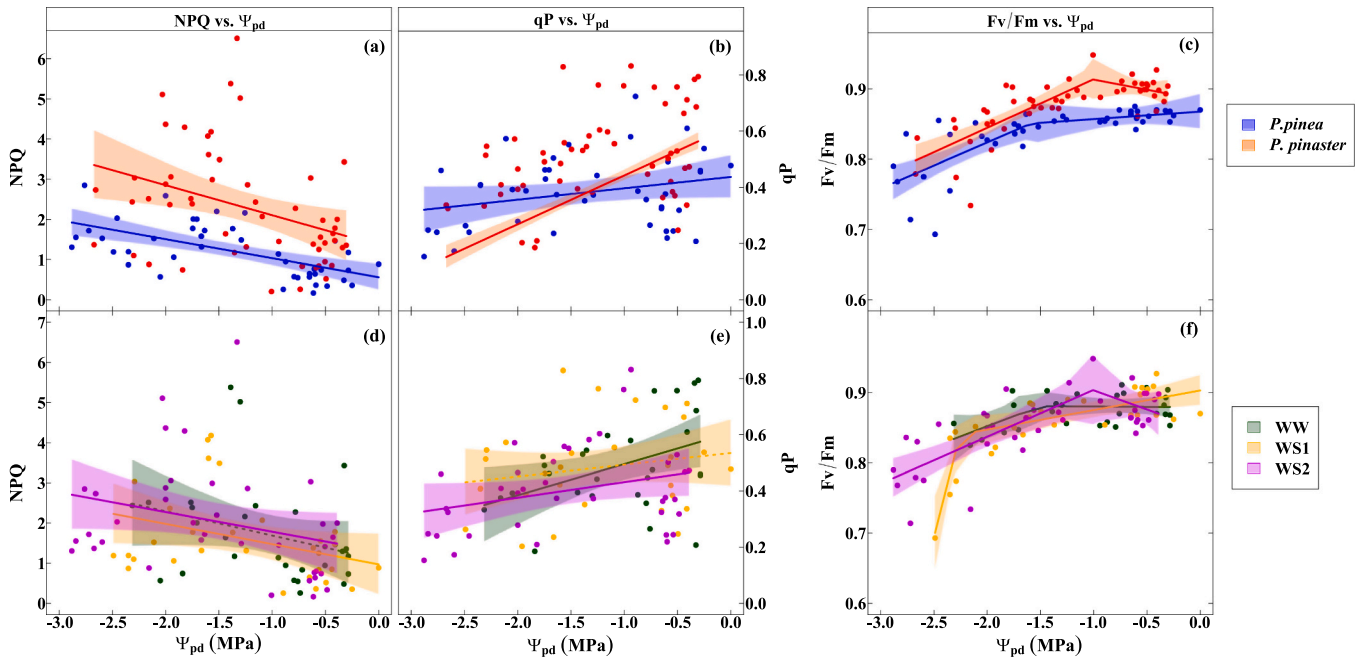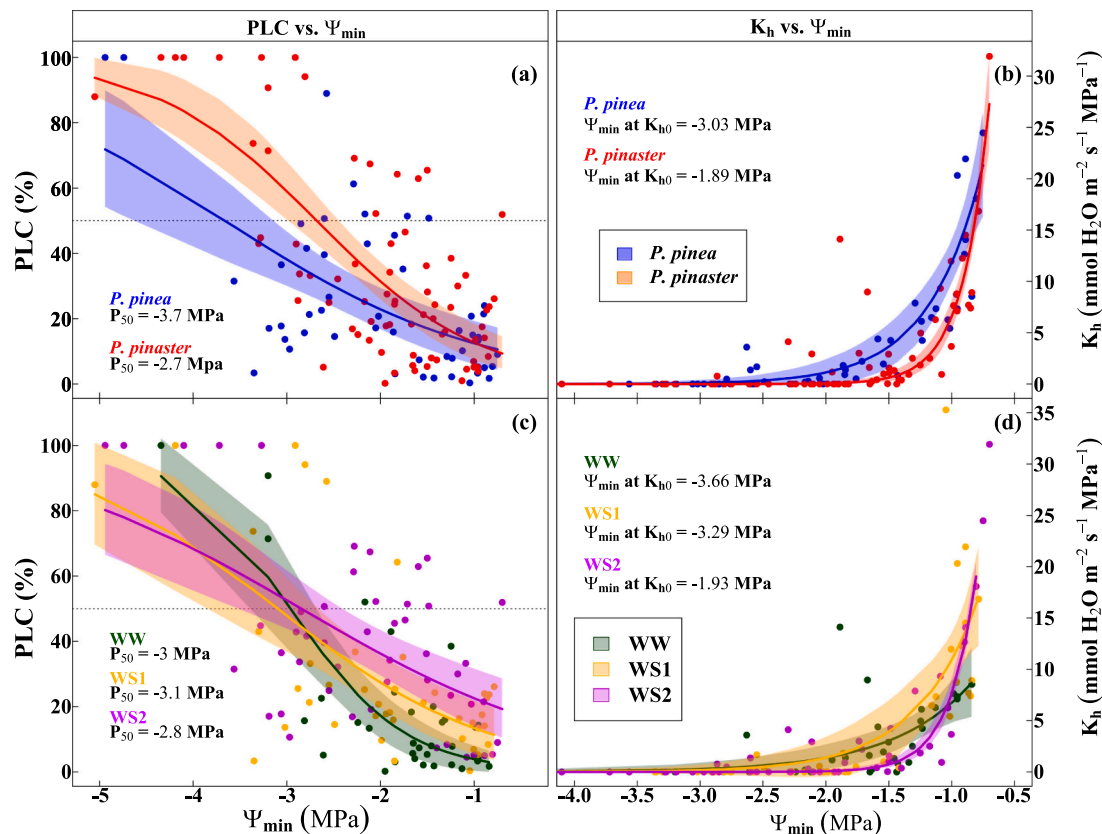

Fig. 3. Non-photochemical quenching (NPQ) (a)-(d), Photochemical Quenching (pQ) (b)-(e), and Fv/Fm (c)-(f) as a function of water stress as measured by predawn water potential (Ψ_{pd}). Non-significant relationships are represented with dashed lines whereas significant relationships with solid lines. Polygons represent 95% confidence intervals for the estimated means.

Fig. 4. Percentage loss conductivity (PLC) and leaf specific apparent hydraulic conductance in the soil–plant–atmosphere continuum (K_h) as functions of midday water potential (Ψ_{min}): (a) and (b) are by species, and (c) and (d) by water stress treatment, respectively. Polygons represent 95% confidence intervals for the estimated means.

$\Psi_{pd} \approx -1$MPa, but thereafter diverged between species: both parameters increased with increasing water stress in *P. pinaster* (i.e. plants weakened their osmotic adjustment capacity), while they decreased in *P. pinea* (Fig. 5c, d). There was no difference among the three pre-WS treatments (i.e. no memory to water stress) for any of the different osmoregulation parameters (Appendix 6).

Finally, as an integration of functional adjustments to define the hydraulic strategy, both species had very small and similar hydroscapes (Fig. 6). Both species being very isohydric, the slightly larger hydroscape in *P. pinea* suggested a comparatively less isohydric behavior than *P. pinaster*.

4. Discussion

High mortality rates in many forests worldwide makes research on the hydraulic and carbon mechanisms explaining drought-induced and heat-induced mortality one of the most urgent matters in global change ecology (Brodribb et al., 2020; Trugman et al., 2021; Hammond et al., 2022; Hartmann et al., 2022; McDowell et al., 2022). Despite expressing isohydric behavior with small hydroscapes (Martínez-Vilalta and Garcia-Forner, 2017; Meinzer et al., 2016; Fu and Meinzer, 2018; Li et al., 2019), the two closely related conifers studied exhibited different physiological performance under increasing water stress driving plants to mortality. Adding to species-specific differences in drought-tolerance and performance under water stress, seedlings carried negative physiological legacies in the hydraulic and carbon functions left by cumulative water stress previous to full watering withdrawal (Anderegg et al., 2013; Wu et al., 2018; Kannenberg et al., 2019a, 2020; Zweifel et al., 2020). Observed differences in the sensitivity to drought of seedlings agree with much scarcer regeneration of *P. pinaster* than *P. pinea* in mixed stands (Gea-Izquierdo et al., 2019; Vergarechea et al., 2019;

Férriz et al., 2021, 2023). Our results suggest that physiological fatigue under cumulative water stress might be a key physiological mechanism predisposing drought-induced mortality in trees (Cailleret et al., 2017; Choat et al., 2018; Gessler et al., 2020; Mantova et al., 2022).

4.1. Drought-tolerance and physiological performance under increasing water stress

The plethora of functional processes regulating the carbon and water balances in plants are linked to the mechanisms governing drought-induced mortality (Adams et al., 2017; Deans et al., 2020; de Kauwe et al., 2022; Joshi et al., 2022; McDowell et al., 2022). Similarly, species drought-tolerance is determined by coordination of different functional traits at different organizational scales (Niinemets and Valladares, 2006; Mencuccini et al., 2015; Bartlett et al., 2016; López et al., 2021). *P. pinea* seedlings were more tolerant to drought than those of *P. pinaster* consistently in both hydraulic and gas exchange traits. *P. pinea* had better hydraulic performance under water stress than *P. pinaster* as expressed among other functional traits by wider hydraulic safety margins and lower P50 (Martínez-Vilalta and Piñol, 2002; Oliveras et al., 2003; Delzon et al., 2010; Battipaglia et al., 2016). *P. pinaster* shows little intraspecific variability in embolism resistance among populations (Corcuera et al., 2011; Lamy et al., 2014), suggesting that homeostasis in plant water status is probably achieved through individual phenotypic plasticity of other coordinated traits (Corcuera et al., 2012; Pivovaroff et al., 2016; Rosas et al., 2019; Fernández-de-Simón et al., 2020). Our P50 estimated using native embolism measurements were higher than those reported for *P. pinaster* by Delzon et al. (2010), Lamy et al. (2014) and Corcuera et al. (2011), but very similar to those reported for the two species by Martínez-Vilalta and Piñol (2002), Oliveras et al. (2003) and Battipaglia et al. (2016). Lower P50 in *P. pinea*
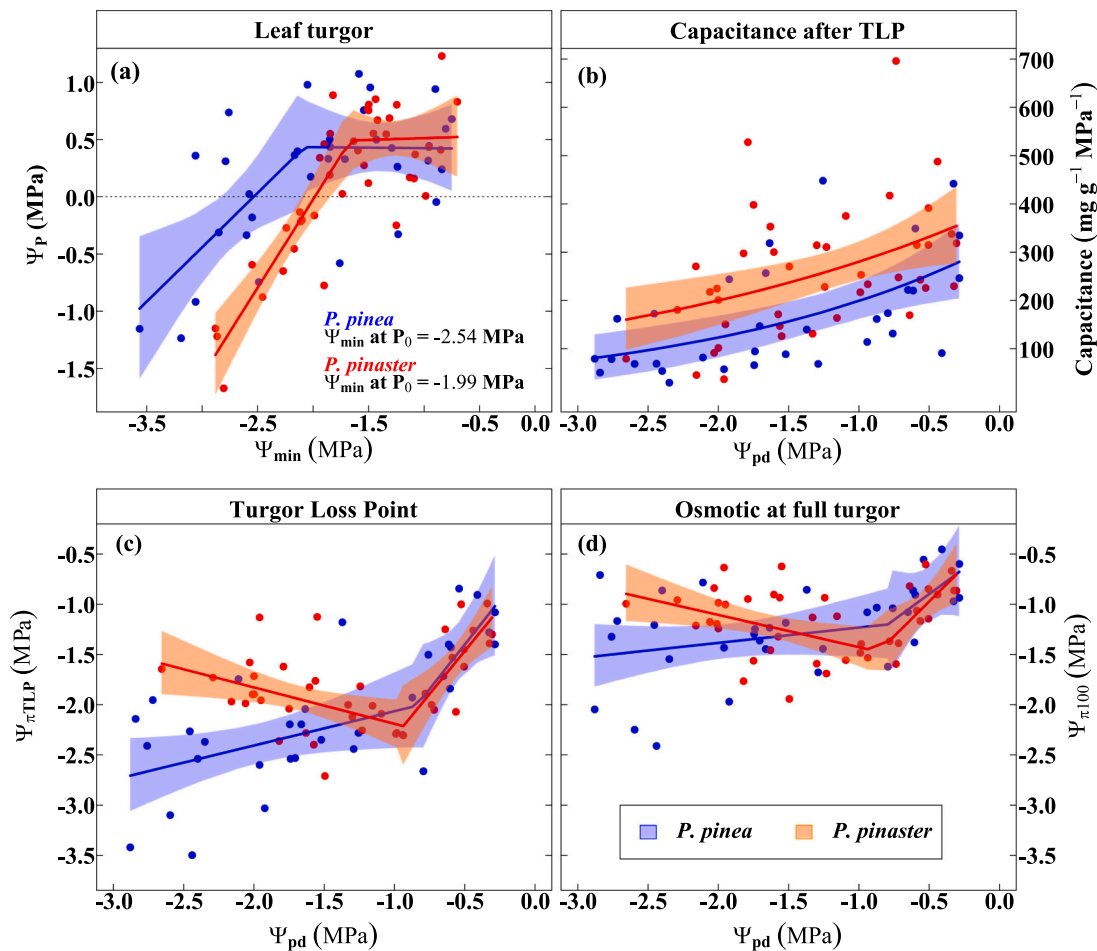
Fig. 5. (a) Leaf hydrostatic pressure (turgor, Ψ_P) as a function of midday water potential (Ψ_{min}); (b) Capacitance after the turgor loss point (TLP), (c) osmotic potential at the turgor loss point ($\Psi_{\pi TLP}$), and (d) osmotic potential at full turgor as a function of predawn leaf water potential (Ψ_{pd}) by species. Negative Ψ_P values in (a) correspond to $\Psi_{min} < \Psi_{\pi TLP}$. Polygons represent 95% confidence intervals for the estimated means.

than *P. pinaster* seems to be a species general pattern, given that P50 can show some intraspecific plasticity (Feng et al., 2023 but see Alon et al., 2023). *P. pinea* also shows higher xylem phenotypic plasticity under water stress than *P. pinaster* (Férriz et al., 2023). Consequently *P. pinea* was able to keep comparatively higher leaf-specific conductivities (Martínez-Vilalta and Piñol, 2002; Corcuera et al., 2011; Poyatos et al., 2013). Both species reached similar maximum A_n, but *P. pinea* achieved greater maximum g_s rates, and exhibited more efficient photoprotection mechanisms, hence suffered less photochemical damage under high water stress (Flexas et al., 2014; Niinemets and Keenan, 2014). Although *P. pinaster* is more efficient using water (Martínez-Vilalta and Piñol, 2002; Corcuera et al., 2012; Medlyn et al., 2017; Férriz et al., 2023), plant carbon and water dynamics were more resistant to water stress in *P. pinea* seedlings.

It is necessary to assess plant vulnerability along the whole stem-leaf hydraulic pathway and the soil-plant-atmosphere continuum to gain a complete understanding of forest dynamics under climate change (Sperry et al., 2015, 2019; Mencuccini et al., 2019; Skelton et al., 2019). *P. pinea* kept higher osmoregulation capacity under high water stress than *P. pinaster*. Plants reached negative leaf turgor under high water stress, which does not seem to be an exception in plants (Charrier, 2020; Knipfer et al., 2020; Ali et al., 2023; Alon et al., 2023). Remarkably, *P. pinaster* was not able to maintain osmoregulation at water potentials below -1.0 MPa. After this threshold, *P. pinaster* seemed to lose or at least weaken its capacity of osmotic adjustment, whereas *P. pinea* maintained it with increasing water stress though at a slower pace. Osmoregulation plays also an important role to understand

non-structural carbohydrate (NSC) dynamics in trees under stress (Martínez-Vilalta et al., 2017; Fernández-de-Simón et al., 2020; Aranda et al., 2021; Arend et al., 2021). Reductions in the carbon balance forced by stress constrain not only primary and secondary growth, but also different metabolic processes highly carbon demanding such as those related to the synthesis of NSC and osmoregulation (Sapes et al., 2021; Thompson et al., 2023). Although a moderate osmotic adjustment capacity linked with specific metabolic changes in response to drought has been reported for both species (Fernández et al., 1999; Nguyen-Queyrens et al., 2002; Nguyen-Queyrens and Bouchet-Lannat, 2003; Deligoz and Gur, 2015; de Miguel et al., 2016; Fernández de Simón et al., 2020), this mechanism was more limited under extremely dry conditions in *P. pinaster* than *P. pinea*. The turgor loss point is intimately connected to the degree of isohidry and associated adjustment of functional traits defining the plant water use strategy (Bartlett et al., 2016; Li et al., 2019; Knipfer et al., 2020; Liang et al., 2021; Salvi et al., 2022). The leaf turgor loss point ($\Psi_{\pi TLP}$) and associated total loss of leaf conductivity have been associated with Ψ_{lethal}. Higher Ψ_{lethal} in leaves than stems can be expected from hydraulic segmentation theory, a strategy that can be employed by plants to protect their hydraulic system (Tyree and Ewers, 1991; Skelton et al., 2019; Charrier, 2020; Brodribb et al., 2020; Lens et al., 2022). A poor capacity of osmoregulation in response to increasing water stress would have strong implications for species capacity to withstand a warmer and drier climate (Lambers et al., 2008; Meinzer et al., 2014; Bartlett et al., 2016; McDowell et al., 2022; Salvi et al., 2022). These results stress the importance of addressing osmoregulation capacity across species as a key trait to buffer
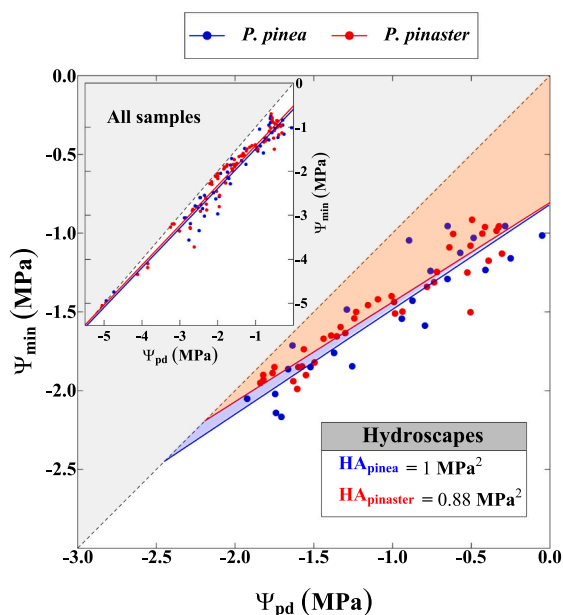
Fig. 6. Predawn (Ψ_{pd}) vs. Midday water potential (Ψ_{min}): (a) all measured potentials, i.e. "Slope all line" (Martínez-Vilalta et al., 2014) with a pseudo-hydroscape calculated as reference; (b) Hydroscapes calculated following Meinzer et al. (2016). Orange polygon=hydroscape *P. pinaster*; orange+blue=hydroscape *P. pinea*.

the negative effects of climate change.

4.2. Memory to cumulative water stress can leave negative physiological legacies

Addressing lagged physiological effects left by cumulative past stress across organizational scales and functional traits in plants is complex. Drought and other abiotic stresses leave legacies in forests, conditioning posterior tree performance under recurrent stress (Anderegg et al., 2013; Wu et al., 2018; Brodribb et al., 2020; Kannenberg et al., 2019a, 2019b; Gessler et al., 2020). Physiological legacies can affect both the water and carbon balances (Anderegg et al., 2013; Skelton et al., 2019; Kannenberg et al., 2020; Zweifel et al., 2020). In our study, physiological memory to previous water stress in the carbon balance affected the gas exchange and photosynthetic efficiency but not the leaf photochemical energy dissipation processes (Niinemets and Keenan, 2014). Seedlings withstanding higher water stress previous to full watering withdrawal (i.e. pre-WS treatment) expressed lower leaf-level water use efficiency (both iWUE and WUE), lower maxima A_n and g_s, with more sensitive stomatal regulation and curtailed photosynthesis under increasing water stress (i. e. lower Ψ). We expected memory effects in the hydraulic function because hydraulic recovery after drought, if existent, requests formation of new conductive area (Skelton et al., 2019; Rehschuh et al., 2020). The water stress levels achieved in the pre-WS treatments were not meant to be extreme compared to those later reached by the plants in the full water deprivation phase at the end of the experiment. Although we observed no legacy effects in osmotic regulation, our plants could have expressed certain degree of hydraulic fatigue as shown by initial PLC above zero and steeper declines in Kh in WS2 plants as a result of the pre-WS treatments. Hydraulic coordination between the stem and the leaf level is complex. Therefore, xylem hydraulic loss in plants can produce long-lasting legacies in the regulation of gas exchange (Skelton et al., 2017; Hammond et al., 2019; Kannenberg et al., 2020; Arend et al., 2021 but see Li et al., 2015). The physiological memory in the carbon function might also be related to quantitative or qualitative reductions in certain metabolites within NSC (Poyatos et al., 2013; Adams et al., 2017; Arend et al., 2021, 2022).

The coordination of functional traits explaining species differences in drought-tolerance was linked to differences in physiological thresholds before mortality. Altogether, our results show that *P. pinea* seedlings died under higher water stress levels (i.e. Ψ_{lethal} was likely reached at higher absolute levels) than *P. pinaster* seedlings. This agrees with our hypothesis that current contrasting adult mortality and regeneration dynamics of these species in mixed stands can be explained by differences in species tolerance to enhanced intensity and duration of drought (Gea-Izquierdo et al., 2019; Férriz et al., 2021, 2023). Additionally, physiological legacies to cumulative water stress might help to explain lagged tree mortality years after drought events in natural populations (Cailleret et al., 2017; Tai et al., 2017; Kannenberg et al., 2020; Gea-Izquierdo et al., 2021; McDowell et al., 2022). The subtle differences observed in the tolerance to drought of the two species suggest that under expected scenarios of increased aridity and further increases in VPD (Lionello and Scarascia, 2018; Grossiord et al., 2020; IPCC et al., 2022), not only the dynamics of *P. pinaster* but also those of *P. pinea* might be jeopardized in the future (Martínez-Vilalta and Lloret, 2016; Sperry et al., 2015, 2019; de Kauwe et al., 2022).

5. Conclusions

The two pine species studied expressed negative physiological legacies of drought and species-specific differences in hydraulic performance, osmotic adjustment and gas exchange under rising water stress. Being both species highly isohydric with very small hydroscapes, *P. pinea* was consistently more tolerant to drought, and comparatively expressed a more anisohydric behavior than *P. pinaster*. Although *P. pinaster* has greater water use efficiency, *P. pinea* can maintain greater performance under water stress expressed by lower xylem conductivity loss, greater photosynthetic and stomatal conductance rates, lower photochemical damage and higher capacity to maintain leaf osmotic adjustment. This shows that *P. pinea* can withstand more severe water stress levels, and therefore should have lower Ψ_{lethal} than *P. pinaster*. Additionally, higher water stress conditions previous to the lethal drought treatment imprinted some physiological legacies in plants including lower water use efficiency (WUE and iWUE) and curtailed photosynthesis capacity with greater stomatal regulation. The lagged physiological legacies in gas exchange of plants forced by a more intense water stress pre-treatment was also expressed by certain degree of hydraulic fatigue with higher PLC and lower leaf specific conductance, but not by changes in osmotic regulation. Extrapolated to field conditions, our results may give insights on the physiological mechanisms and thresholds behind species regeneration dynamics and mortality in mixed stands under climate change.

Declaration of Competing Interest

The authors declare the following financial interests/personal relationships which may be considered as potential competing interests: Guillermo Gea-Izquierdo reports financial support was provided by Ministry of Science Technology and Innovations.

**Data Availability**

Data will be made available on request.

Appendix 1. Illustration of the systematic rule used to select data to calculate the species-specific hydroscape (HA). (a) Sigmoidal relationship calculated between plant water potential (Ψ_{min}) and stomatal conductance (g_s) used to calculate thresholds (α and β) of data used to calculate boundaries of the hydroscape; (b) The hydroscape triangle is depicted in shaded gray color in (b). Red color symbols in (b) are those observations used to calculate the hydroscape boundaries together with the 1:1 line and the y-axis. Data shown are for *Pinus pinaster* and include the black (all observations), red (those defining the hydroscape) and green (those not included in the hydroscape) symbols. Ψ_{pd}= predawn water potential. See Fig. 6 for further interpretation of (b)


.
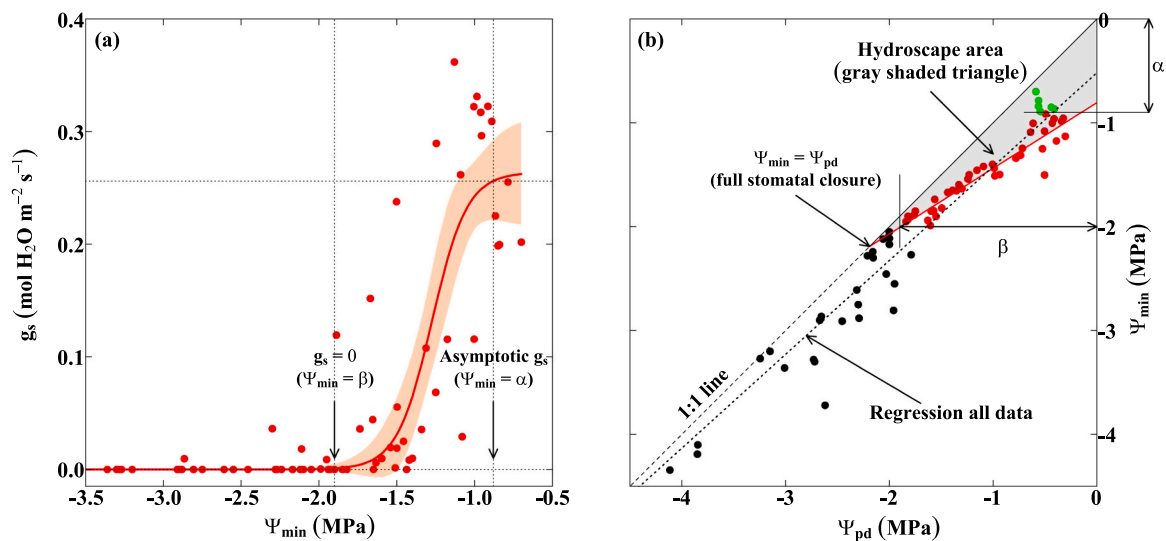
Appendix 2. Non-linear functions used to mimic the studied physiological processes, i.e. bivariate relationships among functional traits and among functional traits and plant water potentials

| Function name	Function	Functional trait		Parameters of physiological interest
		x	**y**	
Piecewise regression	$y = a_1 + b_1 \bullet x$, for x < TP $y = a_2 + b_2 \bullet x$, for x ≥ TP	Ψ_{pd}	F_v/F_m, Ψ_P, $\Psi_{\pi TLP}$, $\Psi_{\pi 100}$	TP=Break or tipping points in linear processes
Asymptotic exponential	$y = a \cdot \left(1 - e^{(-b \cdot x)}\right)$	g_s, E_T	A_n	a = horizontal asymptote, i.e. maximum photosynthesis rate b = function shape-breadth
Sigmoid	$y = a \cdot \left(1 - e^{(-b \cdot x)}\right)^c$	ETR, Ψ_{min}	A_n, g_s	a = horizontal asymptote, i.e. maximum photosynthesis rate or stomatal conductance b = function shape-breadth c = approximate of x at y ≈ 0 (e.g. Ψ_{gs0}) inflection point=log(c)/b
Exponential	$y = a \cdot e^{b \cdot x}$	Ψ_{min}	K_h	a = y(0) b = function shape-breadth

Appendix 3. Photosynthesis as a function of: (a) Leaf transpiration to H_2O (WUE) for the two species. (b) for the three drought legacy treatments
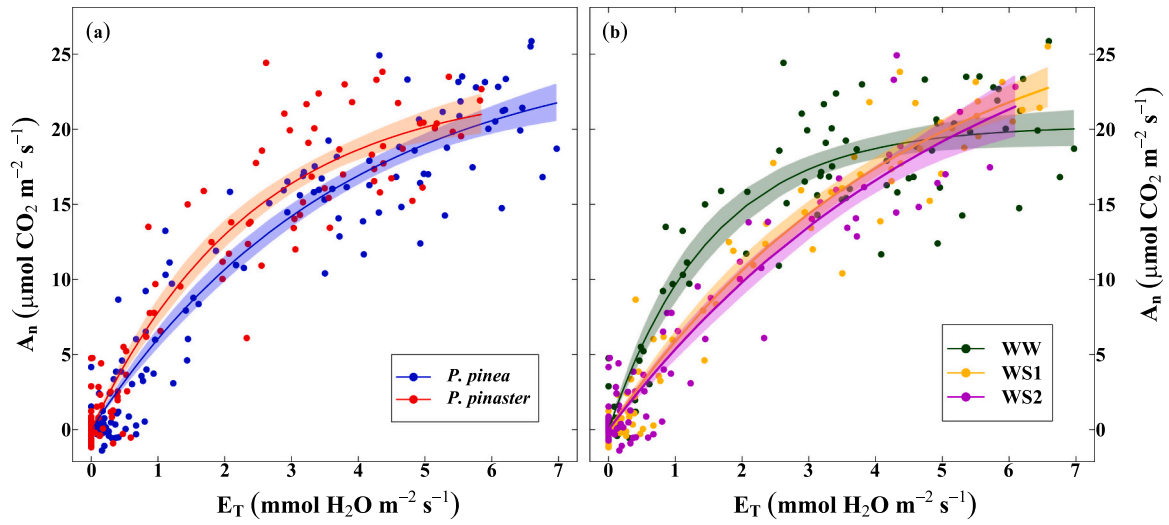
Appendix 4. ETR and Fv'/Fm' as a function of predawn plant water potential (Ψ_{pd}): (a)-(c) by species; (c)-(d) by water stress pre-treatment
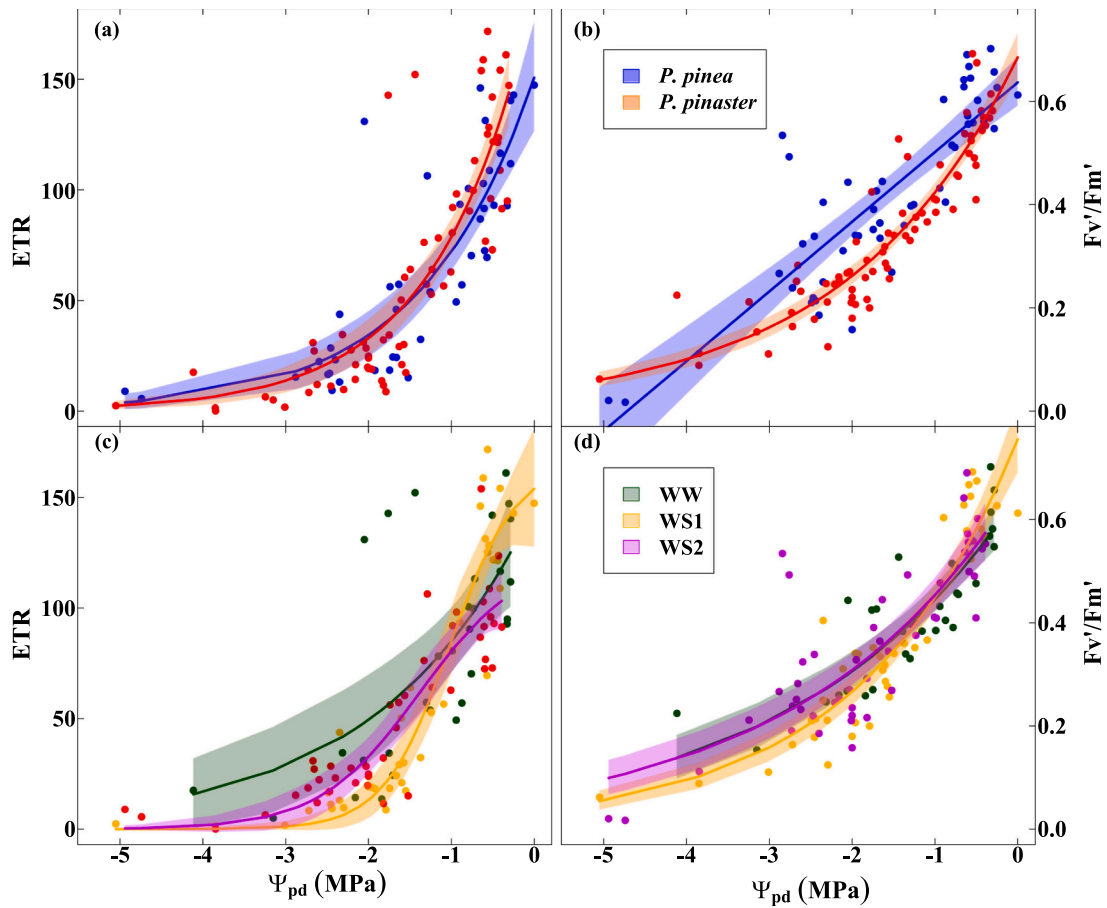
Appendix 5. Percentage loss of conductivity (PLC) as a function of midday water potential (Ψ_{min}) for the different pre-WS treatments. 95% confidence intervals are shown by pre-treatment. Calculated P50 values for the six groups (3 pre-WS, 2 species) are shown. See main text and Fig. 4 for further explanation
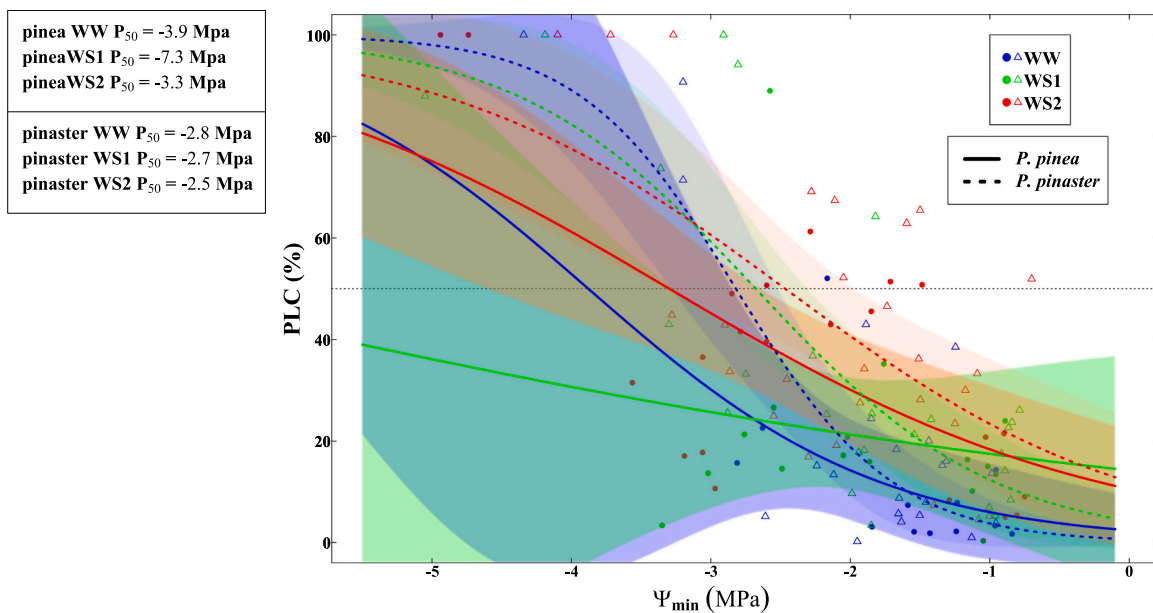
Appendix 6. Same as Fig. 5 but by water treatment instead of by species. (a) Leaf hydrostatic pressure (turgor, Ψ_P); (b) Capacitance after the turgor loss point (TLP); (c) TLP; and (d) osmotic potential at full turgor. (a) is a function of midday water potential (Ψ_{min}), whereas (b) to (d) are functions of predawn water potentials (Ψ_{Pd}) by species. Negative Ψ_P values in (a) correspond to $\Psi_{min} < \Psi\pi_{TLP}$, i.e. conditions were plants theoretically withstood water stress below the turgor loss point
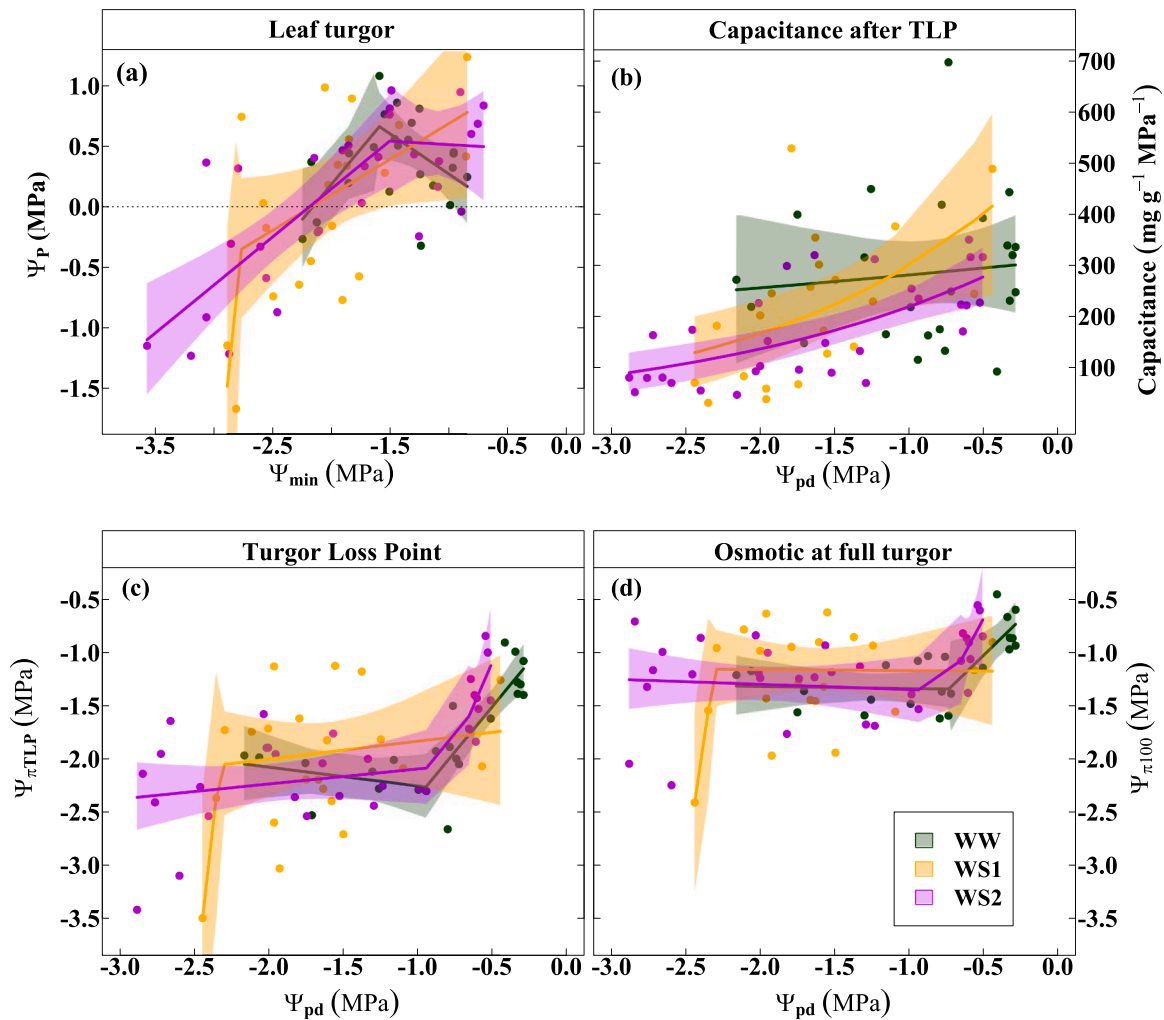
References

Adams, H.D., Zeppel, M.J.B., Anderegg, W.R.L., Hartmann, H., Landhäusser, S.M., Tissue, D.T., McDowell, N.G., 2017. A multi-species synthesis of physiological mechanisms in drought-induced tree mortality. Nat. Ecol. Evol. 1 (9), 1285–1291. https://doi.org/10.1038/s41559-017-0248-x.

Ali, O., Cheddadi, I., Landrein, B., Long, Y., 2023. Revisiting the relationship between turgor pressure and plant cell growth. N. Phytol. 238 (1), 62–69. https://doi.org/10.1111/nph.18683.

Alon, A., Cohen, S., Burlett, R., Hochberg, U., Lukyanov, V., Rog, I., Klein, T., Cochard, H., Delzon, S., David-Schwartz, R., 2023. Acclimation limits for embolism resistance and osmotic adjustment accompany the geographical dry edge of Mediterranean species. Funct. Ecol. https://doi.org/10.1111/1365-2435.14289.

Anderegg, W.R.L., Plavcova, L., Anderegg, L.D.L., Hacke, U.G., Berry, J.A., Field, C.B., 2013. Drought's legacy: multiyear hydraulic deterioration underlies widespread aspen forest die-off and portends increased future risk. Glob. Change Biol. 19 (4), 1188–1196. https://doi.org/10.1111/gcb.12100.

Anderegg, W.R.L., Hicke, J.A., Fisher, R.A., Allen, C.D., Aukema, J., Bentz, B., Hood, S., Lichstein, J.W., Macalady, A.K., Mcdowell, N., Pan, Y., Raffa, K., Sala, A., Shaw, J.D., Stephenson, N.L., Tague, C., Zeppel, M., 2015. Tree mortality from drought, insects, and their interactions in a changing climate. New Phytol. 208 (3), 674–683. https://doi.org/10.1111/nph.13477.

Aranda, I., Gil, L., Pardos, J.A., 2005. Seasonal changes in apparent hydraulic conductance and their implications for water use of European beech (*Fagus sylvatica* L.) and sessile oak [*Quercus petraea* (Matt.) Liebl] in South Europe. Plant Ecol. 179 (2), 155–167. https://doi.org/10.1007/s11258-004-7007-1.

Aranda, I., Cadahía, E., Fernández De Simón, B., 2021. Specific leaf metabolic changes that underlie adjustment of osmotic potential in response to drought by four Quercus species. Tree Physiol. 41 (5), 728–743. https://doi.org/10.1093/treephys/tpaa157.

Arend, M., Link, R.M., Patthey, R., Hoch, G., Schuldt, B., Kahmen, A., 2021. Rapid hydraulic collapse as cause of drought-induced mortality in conifers. Proc. Natl. Acad. Sci. USA 118 (16), 1–6. https://doi.org/10.1073/pnas.2025251118.

Arend, M., Kahmen, A., Link, R.M., Zahnd, C., Schuldt, B., 2022. Lack of hydraulic recovery as a cause of post-drought foliage reduction and canopy decline in European beech. New Phytol. 234, 1195–1205. https://doi.org/10.1111/nph.18065.

Bartlett, M.K., Klein, T., Jansen, S., Choat, B., Sack, L., 2016. The correlations and sequence of plant stomatal, hydraulic, and wilting responses to drought. Proc. Natl. Acad. Sci. USA 113 (46), 13098–13103. https://doi.org/10.1073/pnas.1604088113.

Battipaglia, G., Savi, T., Ascoli, D., Castagneri, D., Esposito, A., Mayr, S., Nardini, A., 2016. Effects of prescribed burning on ecophysiological, anatomical and stem hydraulic properties in Pinus pinea L. Tree Physiol. 36 (8), 1–13. https://doi.org/10.1093/treephys/tpw034.

Beer, C., Ciais, P., Reichstein, M., Baldocchi, D., Law, B.E., Papale, D., Wohlfahrt, G., 2009. Temporal and among-site variability of inherent water use efficiency at the ecosystem level. Glob. Biogeochem. Cycles 23 (2). https://doi.org/10.1029/2008GB003233.

Breshears, D.D., Fontaine, J.B., Ruthrof, K.X., Field, J.P., Feng, X., Burger, J.R., Hardy, G. E.S.J., 2021. Underappreciated plant vulnerabilities to heat waves. New Phytol. 231 (1), 32–39. https://doi.org/10.1111/nph.17348.

Brodribb, T.J., Powers, J., Cochard, H., Choat, B., 2020. Hanging by a thread? Forests and drought. Science 368 (6488), 261–266. https://doi.org/10.1126/science.aat7631.

Cailleret, M., Jansen, S., Robert, E.M.R., Desoto, L., Aakala, T., Antos, J.A., Beikircher, B., Bigler, C., Bugmann, H., Caccianiga, M., Čada, V., Camarero, J.J., Cherubini, P., Cochard, H., Coyea, M.R., Čufar, K., Das, A.J., Davi, H., Delzon, S., Martínez-Vilalta, J., 2017. A synthesis of radial growth patterns preceding tree mortality. Glob. Change Biol. 23 (4), 1675–1690. https://doi.org/10.1111/gcb.13535.

Charrier, G., 2020. Extrapolating physiological response to drought through step-by-step analysis of water potential. In: Plant Physiology, Vol. 184. American Society of Plant Biologists, pp. 560–561. https://doi.org/10.1104/pp.20.01110.

Choat, B., Brodribb, T.J., Brodersen, C.R., Duursma, R.A., López, R., Medlyn, B.E., 2018. Triggers of tree mortality under drought. Nature 558 (7711), 531–539. https://doi.org/10.1038/s41586-018-0240-x.

Cobb, R.C., Ruthrof, K.X., Breshears, D.D., Lloret, F., Aakala, T., Adams, H.D., Anderegg, W.R., Ewers, B.E., Galiano, L.I., Grcunzweig, J.M., Hartmann, H., Huang, C.Y., Klein, T., Kunert, N., Kitzberger, T., Landhcausser, S.M., Levick, S., Preisler, Y., Suarez, M.L., Zeppel, M.J.B., 2017. Ecosystem dynamics and management after forest Die-Off: a global synthesis with conceptual state-and-transition models. Ecosphere 8 (12), e02034. https://doi.org/10.1002/ecs2.2034.

Cochard, H., Badel, E., Herbette, S., Delzon, S., Choat, B., Jansen, S., 2013. Methods for measuring plant vulnerability to cavitation: a critical review. J. Exp. Bot. 64, 4779–4791. https://doi.org/10.1093/jxb/ert193.

Corcuera, L., Cochard, H., Gil-Pelegrín, E., Notivol, E., 2011. Phenotypic plasticity in mesic populations of Pinus pinaster improves resistance to xylem embolism (P50) under severe drought. Trees - Struct. Funct. 25 (6), 1033–1042. https://doi.org/10.1007/s00468-011-0578-2.

Corcuera, L., Gil-Pelegrín, E., Notivol, E., 2012. Differences in hydraulic architecture between mesic and xeric Pinus pinaster populations at the seedling stage. Tree Physiol. 32 (12), 1442–1457. https://doi.org/10.1093/treephys/tps103.

Deans, R.M., Brodribb, T.J., Busch, F.A., Farquhar, G.D., 2020. Optimization can provide the fundamental link between leaf photosynthesis, gas exchange and water relations. Nat. Plants 6 (9), 1116–1125. https://doi.org/10.1038/s41477-020-00760-6.

Deligoz, A., Gur, M., 2015. Morphological, physiological and biochemical responses to drought stress of Stone pine (Pinus pinea L.) seedlings. Acta Physiol. Plant. 37, 243. https://doi.org/10.1007/s11738-015-1998-1.

Delzon, S., Douthe, C., Sala, A., Cochard, H., 2010. Mechanism of water-stress induced cavitation in conifers: Bordered pit structure and function support the hypothesis of seal capillary-seeding. Plant, Cell Environ. 33 (12), 2101–2111. https://doi.org/10.1111/j.1365-3040.2010.02208.x.

Feng, F., Wagner, Y., Klein, T., Hochberg, U., 2023. Xylem resistance to cavitation increases during summer in Pinus halepensis. Plant Cell Environ. https://doi.org/10.1111/pce.14573.

Fernández, M., Gil, L., Pardos, J.A., 1999. Response of Pinus pinaster Ait. provenances at early age to water supply. I. Water relation parameters. Ann. For. Sci. 56 (2), 179–187.

Fernández-de-Simón, B., Sanz, M., Sánchez-Gómez, D., Cadahía, E., Aranda, I., 2020. Rising [CO2] effect on leaf drought-induced metabolome in Pinus pinaster Aiton: ontogenetic- and genotypic-specific response exhibit different metabolic strategies. Plant Physiol. Biochem. 149, 201–216. https://doi.org/10.1016/j.plaphy.2020.02.011.

Férriz, M., Martin-Benito, D., Cañellas, I., Gea-Izquierdo, G., 2021. Sensitivity to water stress drives differential decline and mortality dynamics of three co-occurring conifers with different drought tolerance. For. Ecol. Manag. 486 https://doi.org/10.1016/j.foreco.2021.118964.

Férriz, M., Martin-Benito, D., Fernández-de-Simón, M.B., Conde, M., García-Cervigón, A. I., Aranda, I., Gea-Izquierdo, G., 2023. Forest disturbances and climate constrain carbon allocation dynamics in trees. Tree Physiol. 43 (6), 909–924. https://doi.org/10.1093/treephys/tpad021.

Flexas, J., Diaz-Espejo, A., Gago, J., Gallé, A., Galmés, J., Gulías, J., Medrano, H., 2014. Photosynthetic limitations in Mediterranean plants: A review. Environ. Exp. Bot. 103, 12–23. https://doi.org/10.1016/j.envexpbot.2013.09.002.

Fu, X., Meinzer, F.C., 2018. Metrics and proxies for stringency of regulation of plant water status (iso/anisohydry): A global data set reveals coordination and trade-offs among water transport traits. Tree Physiol. 39 (1), 122–134. https://doi.org/10.1093/treephys/tpy087.

Gea-Izquierdo, G., Férriz, M., García-Garrido, S., Aguín, O., Elvira-Recuenco, M., Hernandez-Escribano, L., Martin-Benito, D., Raposo, R., 2019. Synergistic abiotic and biotic stressors explain widespread decline of Pinus pinaster in a mixed forest. Sci. Total Environ. 685, 963–975. https://doi.org/10.1016/j.scitotenv.2019.05.378.

Gea-Izquierdo, G., Natalini, F., Cardillo, E., 2021. Holm oak death is accelerated but not sudden and expresses drought legacies. Sci. Total Environ. 754 https://doi.org/10.1016/j.scitotenv.2020.141793.

Gessler, A., Bottero, A., Marshall, J., Arend, M., 2020. The way back: recovery of trees from drought and its implication for acclimation. N. Phytol. 228 (6), 1704–1709. https://doi.org/10.1111/nph.16703.

Grossiord, C., Buckley, T.N., Cernusak, L.A., Novick, K.A., Poulter, B., Siegwolf, R.T.W., Sperry, J.S., McDowell, N.G., 2020. Plant responses to rising vapor pressure deficit. In: New Phytologist, Vol. 226. Blackwell Publishing Ltd, pp. 1550–1566. https://doi.org/10.1111/nph.16485.

Hammond, W.M., Yu, K., Wilson, L.A., Will, R.E., Anderegg, W.R.L., Adams, H.D., 2019. Dead or dying? Quantifying the point of no return from hydraulic failure in drought-induced tree mortality. New Phytol. 223 (4), 1834–1843. https://doi.org/10.1111/nph.15922.

Hammond, W.M., Williams, A.P., Abatzoglou, J.T., Adams, H.D., Klein, T., López, R., Sáenz-Romero, C., Hartmann, H., Breshears, D.D., Allen, C.D., 2022. Global field observations of tree die-off reveal hotter-drought fingerprint for Earth's forests. Nat. Commun. 13 (1), 1761. https://doi.org/10.1038/s41467-022-29289-2.

Hartmann, H., Bastos, A., Das, A.J., Esquivel-muelbert, A., Hammond, W.M., Martínez-vilalta, J., Mcdowell, N.G., Powers, J.S., Pugh, T.A.M., Ruthrof, K.X., Allen, C.D., 2022. Climate change risks to global forest health: emergence of unexpected events of elevated tree mortality worldwide. Annu. Rev. Plant Biol. 73, 673–702. https://doi.org/10.1146/annurev-arplant-102820-012804.

Hochberg, U., Rockwell, F.E., Holbrook, N.M., Cochard, H., 2018. Iso / anisohydry: a plant – environment interaction rather than a simple hydraulic trait. Trends Plant Sci. 23 (2), 112–120. https://doi.org/10.1016/j.tplants.2017.11.002.

Hudson, P.J., Limousin, J.M., Krofcheck, D.J., Boutz, A.L., Pangle, R.E., Gehres, N., McDowell, N.G., Pockman, W.T., 2018. Impacts of long-term precipitation manipulation on hydraulic architecture and xylem anatomy of piñon and juniper in Southwest USA. Plant Cell Environ. 41 (2), 421–435. https://doi.org/10.1111/pce.13109.

IPCC, 2022. Climate Change 2022: Impacts, Adaptation, and Vulnerability. In: Pörtner, H.-O., Roberts, D.C., Tignor, M., Poloczanska, E.S., Mintenbeck, K., Alegría, A., Craig, M., Langsdorf, S., Löschke, S., Möller, V., Okem, A., Rama, B. (Eds.), Contribution of Working Group II to the Sixth Assessment Report of the Intergovernmental Panel on Climate Change. Cambridge University Press. Cambridge University Press, Cambridge, UK and New York, NY, USA, p. 3056. https://doi.org/10.1017/9781009325844.

Jacobsen, A.L., Pratt, R.B., 2018. Extensive drought-associated plant mortality as an agent of type-conversion in chaparral shrublands. N. Phytol. 219 (2), 498–504. https://doi.org/10.1111/nph.15186.

Johnson, D.M., Domec, J.C., Carter Berry, Z., Schwantes, A.M., McCulloh, K.A., Woodruff, D.R., Jackson, R.B., 2018. Co-occurring woody species have diverse hydraulic strategies and mortality rates during an extreme drought. Plant Cell Environ. 41 (3), 576–588. https://doi.org/10.1111/pce.13121.

Joshi, J., Stocker, B.D., Hofhansl, F., Zhou, S., Dieckmann, U., Prentice, I.C., 2022. Towards a unified theory of plant photosynthesis and hydraulics (https://do.). Nat. Plants. https://doi.org/10.1101/2020.12.17.423132.

Kannenberg, S.A., Novick, K.A., Alexander, M.R., Maxwell, J.T., Moore, D.J.P., Phillips, R.P., Anderegg, W.R.L., 2019a. Linking drought legacy effects across scales: from leaves to tree rings to ecosystems. Glob. Change Biol. 25 (9), 2978–2992. https://doi.org/10.1111/gcb.14710.

Kannenberg, S.A., Maxwell, J.T., Pederson, N., D'Orangeville, L., Ficklin, D.L., Phillips, R.P., 2019b. Drought legacies are dependent on water table depth, wood anatomy and drought timing across the eastern US. Ecol. Lett. 22 (1), 119–127. https://doi.org/10.1111/ele.13173.

Kannenberg, S.A., Schwalm, C.R., Anderegg, W.R.L., 2020. Ghosts of the past: how drought legacy effects shape forest functioning and carbon cycling. Ecol. Lett. 23 (5), 891–901. https://doi.org/10.1111/ele.13485.

de Kauwe, M.G., Sabot, M.E.B., Medlyn, B.E., Pitman, A.J., Meir, P., Cernusak, L.A., Gallagher, R. v, Ukkola, A.M., Rifai, S.W., Choat, B., 2022. Towards species-level forecasts of drought-induced tree mortality risk. New Phytol. 235 (1), 94–110. https://doi.org/10.1111/nph.18129.

Klein, T., 2014. The variability of stomatal sensitivity to leaf water potential across tree species indicates a continuum between isohydric and anisohydric behaviours. Funct. Ecol. 28 (6), 1313–1320. https://doi.org/10.1111/1365-2435.12289.

Knipfer, T., Bambach, N., Isabel Hernandez, M., Bartlett, M.K., Sinclair, G., Duong, F., Kluepfel, D.A., McElrone, A.J., 2020. Predicting stomatal closure and turgor loss in woody plants using predawn and midday water potential. Plant Physiol. 184 (2), 881–894. https://doi.org/10.1104/pp.20.00500.

Lambers, H., Chapin, F.S., Pons, T.L., 2008. Plant Physiological Ecology, second ed. Springer.

Lamy, J.B., Delzon, S., Bouche, P.S., Alia, R., Vendramin, G.G., Cochard, H., Plomion, C., 2014. Limited genetic variability and phenotypic plasticity detected for cavitation resistance in a Mediterranean pine. N. Phytol. 201 (3), 874–886. https://doi.org/10.1111/nph.12556.

Lens, F., Gleason, S.M., Bortolami, G., Brodersen, C., Delzon, S., Jansen, S., 2022. Functional xylem characteristics associated with drought-induced embolism in angiosperms. New Phytol. https://doi.org/10.1111/nph.18447.

Li, S., Feifel, M., Karimi, Z., Schuldt, B., Choat, B., Jansen, S., 2015. Leaf gas exchange performance and the lethal water potential of five European species during drought. Tree Physiol. tpv117. https://doi.org/10.1093/treephys/tpv117.

Li, X., Blackman, C.J., Peters, J.M.R., Choat, B., Rymer, P.D., Medlyn, B.E., Tissue, D.T., 2019. More than iso/anisohydry:hydroscapes integrate plant water use and drought tolerance traits in 10 eucalypt species from contrasting climates. Funct. Ecol. 33 (6), 1035–1049. https://doi.org/10.1111/1365-2435.13320.

Liang, X., Ye, Q., Liu, H., Brodribb, T.J., 2021. Wood density predicts mortality threshold for diverse trees. N. Phytol. 229 (6), 3053–3057. https://doi.org/10.1111/nph.17117.

Lionello, P., Scarascia, L., 2018. The relation between climate change in the Mediterranean region and global warming. Reg. Environ. Change 18 (5), 1481–1493. https://doi.org/10.1007/s10113-018-1290-1.

López, R., Cano, F.J., Martin-StPaul, N.K., Cochard, H., Choat, B., 2021. Coordination of stem and leaf traits define different strategies to regulate water loss and tolerance ranges to aridity. New Phytol. 230 (2), 497–509. https://doi.org/10.1111/nph.17185.

Mantova, M., Herbette, S., Cochard, H., Torres-Ruiz, J.M., 2022. Hydraulic failure and tree mortality: from correlation to causation. Trends Plant Sci. 27 (4), 335–345. https://doi.org/10.1016/j.tplants.2021.10.003.

Martínez-Vilalta, J., Garcia-Forner, N., 2017. Water potential regulation, stomatal behaviour and hydraulic transport under drought: deconstructing the iso/anisohydric concept. Plant, Cell Environ. 40, 962–976. https://doi.org/10.1111/pce.12846.

Martínez-Vilalta, J., Lloret, F., 2016. Drought-induced vegetation shifts in terrestrial ecosystems: the key role of regeneration dynamics. In: Global and Planetary Change, Vol. 144. Elsevier B.V., pp. 94–108. https://doi.org/10.1016/j.gloplacha.2016.07.009

Martínez-Vilalta, J., Piñol, J., 2002. Drought-induced mortality and hydraulic architecture in pine populations of the NE Iberian Peninsula. For. Ecol. Manag. 161, 247–256. https://doi.org/10.1016/S0378-1127(01)00495-9.

Martínez-Vilalta, J., Poyatos, R., Aguadé, D., Retana, J., Mencuccini, M., 2014. A new look at water transport regulation in plants. New Phytol. 204, 105–115. https://doi.org/10.1111/nph.12912.

Martínez-Vilalta, J., Salas, A., Asensio, D., Galiano, Lu, Hoch, G.ü, Palacio, S., Piper, F.I., Lloret, F., 2016. Dynamics of non- structural carbohydrates in terrestrial plants: a global synthesis. Ecol. Monogr. 86 (4), 495–516. https://doi.org/10.1002/ecm.1231.

Maxwell, K., Johnson, G.N., 2000. Chlorophyll fluorescence-a practical guide. J. Exp. Bot. 51 (345), 659–668. https://doi.org/10.1093/jexbot/51.345.659.

McDowell, N.G., Allen, C.D., Anderson-Teixeira, K., Aukema, B.H., Bond- Lamberty, B., Chini, L., Xu, C., 2020. Pervasive shifts in forest dynamics in a changing world. Science 368 (6494). https://doi.org/10.1126/science.aaz9463.

McDowell, N.G., Sapes, G., Pivovaroff, A., Adams, H.D., Allen, C.D., Anderegg, W.R.L., Xu, C., 2022. Mechanisms of woody-plant mortality under rising drought, CO_2 and vapour pressure deficit. Nat. Rev. Earth Environ. 3 (5), 294–308. https://doi.org/10.1038/s43017-022-00272-1.

Medlyn, B.E., De Kauwe, M.G., Lin, Y.S., Knauer, J., Duursma, R.A., Williams, C.A., Wingate, L., 2017. How do leaf and ecosystem measures of water-use efficiency compare? New Phytol. https://doi.org/10.1111/nph.14626.

Meinzer, F.C., Johnson, D.M., Lachenbruch, B., McCulloh, K.A., Woodruff, D.R., 2009. Xylem hydraulic safety margins in woody plants: coordination of stomatal control of xylem tension with hydraulic capacitance. Funct. Ecol. 23 (5), 922–930. https://doi.org/10.1111/j.1365-2435.2009.01577.x.

Meinzer, F.C., Woodruff, D.R., Marias, D.E., Mcculloh, K.A., Sevanto, S., 2014. Dynamics of leaf water relations components in co-occurring iso- and anisohydric conifer species. Plant Cell Environ. 37 (11), 2577–2586. https://doi.org/10.1111/pce.12327.

Meinzer, F.C., Woodruff, D.R., Marias, D.E., Smith, D.D., McCulloh, K.A., Howard, A.R., Magedman, A.L., 2016. Mapping 'hydroscapes' along the iso- to anisohydric continuum of stomatal regulation of plant water status. Ecol. Lett. 19, 1343–1352. https://doi.org/10.1111/ele.12670.

Melcher, P.J., Holbrook, N.M., Burns, M.J., Zwieniecki, M.A., Cobb, A.R., Brodribb, T.J., Choat, B., Sack, L., 2012. Measurements of stem xylem hydraulic conductivity in the laboratory and field. Methods Ecol. Evol. 3, 685–694. https://doi.org/10.1111/j.2041-210X.2012.00204.x.

Mencuccini, M., Minunno, F., Salmon, Y., Martínez-Vilalta, J., Hölttä, T., 2015. Coordination of physiological traits involved in drought-induced mortality of woody plants. New Phytol. 208 (2), 396–409. https://doi.org/10.1111/nph.13461.

Mencuccini, M., Manzoni, S., Christoffersen, B., 2019. Modelling water fluxes in plants: from tissues to biosphere. N. Phytol. 222 (3), 1207–1222. https://doi.org/10.1111/nph.15681.

de Miguel, M., Guevara, M.Á., Sánchez-Gómez, D., De María, N., Díaz, L.M., Mancha, J.A., Cervera, M.T., 2016. Organ-specific metabolic responses to drought in Pinus pinaster Ait. Plant Physiol. Biochem. 102, 17–26. https://doi.org/10.1016/j.plaphy.2016.02.013.

Nguyen-Queyrens, A., Bouchet-Lannat, F., 2003. Osmotic adjustment in three-year-old seedlings of five provenances of maritime pine (Pinus pinaster) in response to drought. Tree Physiol 23 (6), 397–404. https://doi.org/10.1093/treephys/23.6.397.

Nguyen-Queyrens, A., Costa, P., Loustau, D., Plomion, C., 2002. Osmotic adjustment in Pinus pinaster cuttings in response to a soil drying cycle. Ann. For. Sci. 59 (7), 795–799. https://doi.org/10.1051/forest:2002067.

Niinemets, Ü., Keenan, T., 2014. Photosynthetic responses to stress in Mediterranean evergreens: Mechanisms and models. Environ. Exp. Bot. 103, 24–41. https://doi.org/10.1016/j.envexpbot.2013.11.008.

Niinemets, Ü., Valladares, F., 2006. Tolerance to Shade, Drought, and Waterlogging of Temperate Northern Hemisphere Trees and Shrubs. Ecol. Monogr. 76 (4), 521–547.

Nobel, P.S., 2009. Physicochemical and Environmental Plant Physiology, fourth ed. Academic Press, Elsevier, Oxford UK, p. 568.

Oliveras, I., Martínez-Vilalta, J., Jimenez-Ortiz, T., Lledó, M.J., Escarré, A., Piñol, J., 2003. Hydraulic properties of Pinus halepensis, Pinus pinea and Tetraclinis articulata in a dune ecosystem of Eastern Spain. Plant Ecol. 169 (1), 131–141. https://doi.org/10.1023/A:1026223516580.

Pammenter, N.W., Vander Willigen, C., 1998. A mathematical and statistical analysis of the curves illustrating vulnerability of xylem to cavitation. Tree Physiol 18, 589–593. https://doi.org/10.1093/treephys/18.8-9.589.

Pivovaroff, A.L., Pasquini, S.C., Guzman, M.E., De, Alstad, K.P., Stemke, J.S., Santiago, L.S., 2016. Multiple strategies for drought survival among woody plant species. Funct. Ecol. 30 (4), 517–526. https://doi.org/10.1111/1365-2435.12518.

Poyatos, R., Aguadé, D., Galiano, L., Mencuccini, M., Martínez-Vilalta, J., 2013. Drought-induced defoliation and long periods of near-zero gas exchange play a key role in accentuating metabolic decline of Scots pine. New Phytol. 200 (2), 388–401. https://doi.org/10.1111/nph.12278.

R Core Team, 2020. R: A Language and Environment for Statistical Computing. R Foundation for Statistical Computing, Vienna, Austria (URL). ⟨https://www.R-project.org/⟩.

Rehschuh, R., Cecilia, A., Zuber, M., Faragó, T., Baumbach, T., Hartmann, H., Ruehr, N., 2020. Drought-induced xylem embolism limits the recovery of leaf gas exchange in scots pine. Plant Physiol. 184 (2), 852–864. https://doi.org/10.1104/pp.20.00407.

Robichaux, R.H., 1984. Variation in the tissue water relations of two sympatric Hawaiian Dubautia species and their natural hybrid. Oecologia 59, 344–350. https://doi.org/10.1007/BF00384465.

Rosas, T., Mencuccini, M., Barba, J., Cochard, H., Saura-Mas, S., Martínez-Vilalta, J., 2019. Adjustments and coordination of hydraulic, leaf and stem traits along a water availability gradient. N. Phytol. 223, 632–646. https://doi.org/10.1111/nph.15684.

Salvi, A.M., Gosetti, S.G., Smith, D.D., Adams, M.A., Givnish, T.J., McCulloh, K.A., 2022. Hydroscapes, hydroscape plasticity and relationships to functional traits and mesophyll photosynthetic sensitivity to leaf water potential in Eucalyptus species. Plant Cell Environ. 45 (9), 2573–2588. https://doi.org/10.1111/pce.14380.

Sapes, G., Demaree, P., Lekberg, Y., Sala, A., 2021. Plant carbohydrate depletion impairs water relations and spreads via ectomycorrhizal networks. New Phytol. 229 (6), 3172–3183. https://doi.org/10.1111/nph.17134.

Schindelin, J., Arganda-Carreras, I., Frise, E., Kaynig, V., Longair, M., Pietzsch, T., Cardona, A., 2012. Fiji: an open-source platform for biological-image analysis. Nat. Methods 9 (7), 676–682. https://doi.org/10.1038/nmeth.2019.

Shriver, R.K., Yackulic, C.B., Bell, D.M., Bradford, J.B., 2022. Dry forest decline is driven by both declining recruitment and increasing mortality in response to warm, dry conditions. Glob. Ecol. Biogeogr. (July), 2259–2269. https://doi.org/10.1111/geb.13582.

Skelton, R.P., Brodribb, T.J., McAdam, S.A.M., Mitchell, P.J., 2017. Gas exchange recovery following natural drought is rapid unless limited by loss of leaf hydraulic conductance: evidence from an evergreen woodland. N. Phytol. 215 (4), 1399–1412. https://doi.org/10.1111/nph.14652.

Skelton, R.P., Anderegg, L.D.L., Papper, P., Reich, E., Dawson, T.E., Kling, M., Thompson, S.E., Diaz, J., Ackerly, D.D., 2019. No local adaptation in leaf or stem xylem vulnerability to embolism, but consistent vulnerability segmentation in a North American oak. N. Phytol. 223 (3), 1296–1306. https://doi.org/10.1111/nph.15886.

Sperry, J.S., Love, D.M., 2015. What plant hydraulics can tell us about responses to climate-change droughts. *New Phytol.* Vol. 207 (Issue 1), 14–27. https://doi.org/10.1111/nph.13354.

Sperry, J.S., Venturas, M.D., Todd, H.N., Trugman, A.T., Anderegg, W.R.L., Wang, Y., Tai, X., 2019. The impact of rising CO_2 and acclimation on the response of US forests to global warming. Proc. Natl. Acad. Sci. USA 116 (51), 25734–25744. https://doi.org/10.1073/pnas.1913072116.

Tai, X., Mackay, D.S., Anderegg, W.R.L., Sperry, J.S., Brooks, P.D., 2017. Plant hydraulics improves and topography mediates prediction of aspen mortality in southwestern USA. N. Phytol. 213 (1), 113–127. https://doi.org/10.1111/nph.14098.

Thompson, R.A., Adams, H.D., Breshears, D.D., Collins, A.D., Dickman, L.T., Grossiord, C., Manrique-Alba, À., Peltier, D.M., Ryan, M.G., Trowbridge, A.M., McDowell, N.G., 2023. No carbon storage in growth-limited trees in a semi-arid woodland. Nat. Commun 14 (1), 1959. https://doi.org/10.1038/s41467-023-37577-8.

Trugman, A.T., Anderegg, L.D.L., Anderegg, W.R.L., Das, A.J., Stephenson, N.L., 2021. Why is tree drought mortality so hard to predict? Trends Ecol. Evol. 36 (6), 520–532. https://doi.org/10.1016/j.tree.2021.02.001.

Tyree, M.T., Ewers, F.W., 1991. The hydraulic architecture of trees and other woody-plants. New Phytol. 119 (3), 345–360. https://doi.org/10.1111/j.1469-8137.1991.tb00035.x.

Vergarechea, M., del Río, M., Gordo, J., Martín, R., Cubero, D., Calama, R., 2019. Spatio-temporal variation of natural regeneration in *Pinus pinea* and *Pinus pinaster* Mediterranean forests in Spain. Eur. J. For. Res. 138 (2), 313–326. https://doi.org/10.1007/s10342-019-01172-8.

Woodruff, D.R., Meinzer, F.C., Marias, D.E., Sevanto, S., Jenkins, M.W., Mcdowell, N.G., 2015. Linking nonstructural carbohydrate dynamics to gas exchange and leaf hydraulic behavior in Pinus edulis and Juniperus monosperma. New Phytol. 206 (1), 411–421. https://doi.org/10.1111/nph.13170.

Wu, X., Liu, H., Li, X., Ciais, P., Babst, F., Guo, W., Zhang, C., Magliulo, V., Pavelka, M., Liu, S., Huang, Y., Wang, P., Shi, C., Ma, Y., 2018. Differentiating drought legacy effects on vegetation growth over the temperate Northern Hemisphere. Glob. Change Biol. 24 (1), 504–516. https://doi.org/10.1111/gcb.13920.

Zandalinas, S.I., Mittler, R., 2022. Plant responses to multifactorial stress combination. New Phytol 234, 1161–1167. https://doi.org/10.1111/nph.18087.

Zhou, S., Duursma, R.A., Medlyn, B.E., Kelly, J.W.G., Prentice, I.C., 2013. How should we model plant responses to drought? An analysis of stomatal and non-stomatal responses to water stress. Agric. For. Meteorol. 182–183, 204–214. https://doi.org/10.1016/j.agrformet.2013.05.009.

Zweifel, R., Etzold, S., Sterck, F., Gessler, A., Anfodillo, T., Mencuccini, M., von Arx, G., Lazzarin, M., Haeni, M., Feichtinger, L., Meusburger, K., Knuesel, S., Walthert, L., Salmon, Y., Bose, A.K., Schoenbeck, L., Hug, C., de Girardi, N., Giuggiola, A., Rigling, A., 2020. Determinants of legacy effects in pine trees – implications from an irrigation-stop experiment. New Phytol 227 (4), 1081–1096. https://doi.org/10.1111/nph.16582.